Carbohydrate Polymers 83 (2011) 1541–1546

Contents lists available at ScienceDirect

Carbohydrate Polymers

journal homepage: www.elsevier.com/locate/carbpol

Preparation, structure and crystallinity of chitosan nano-fibers by a solid–liquid phase separation technique

Jianhao Zhao[a,b], Wanqing Han[a], Haodong Chen[a], Mei Tu[a,b,*], Rong Zeng[a,b], Yunfeng Shi[c], Zhengang Cha[b,d], Changren Zhou[a,b]

[a] Department of Materials Science and Engineering, College of Science and Engineering, Jinan University, Guangzhou 510632, China
[b] Engineering Research Center of Artificial Organs and Materials, Ministry of Education, Guangzhou 510632, China
[c] Analysis and Test Center, Jinan University, Guangzhou 510632, China
[d] Department of Orthopaedics, First Hospital Attached to Jinan University, Guangzhou 510632, China

ARTICLE INFO

Article history:
Received 2 September 2010
Received in revised form
27 September 2010
Accepted 1 October 2010
Available online 12 October 2010

Key words:
Chitosan
Nano-fibrous
Solid–liquid phase separation
Structure
Crystallinity

ABSTRACT

Chitosan acetate nano-fibers were fabricated via a solid–liquid phase separation technique. The chitosan acetate structure was influenced by phase separation temperature, chitosan concentration and acetic acid concentration. Uniform nano-fibrous chitosan acetate of 50–500 nm in diameter was engineered at 0.05% (w/v) chitosan and 0.025% (v/v) acetic acid in liquid nitrogen, as opposed to film-shape and micro-fibrous structure at −18 °C and −80 °C respectively. Decreasing the chitosan concentration led to the formation of nano-fibrous/floccules-like structure, while increasing the acetic acid concentration resulted in nano-/micro-fibrous structure instead. The chitosan acetate structure was closely related to the crystallinity varying with different phase separation conditions. Nano-fibrous chitosan acetate showed a medium crystallinity with a glass transition temperature of 155.1 °C and a heat capacity of 29.1 J/g comparing with nano-fibrous/floccules-like and nano-/micro-fibrous samples. The chitosan acetate crystal was also found changeable from form I to form II after solid–liquid phase separation in liquid nitrogen.

1. Introduction

Conventionally, fibers having diameters less than 1 μm would be classified as nano-fibers. Due to their small scale in diameter, nano-fibrous materials have a very high surface-to-volume ratio, which makes them very good candidates for the delivery of bioactive agents as well as the tissue engineering matrices (Sahoo, Ang, Goh, & Toh, 2010; Wei & Ma, 2008; Zhao, Tanaka, Kinoshita, Higuchi, & Tan, 2010). Nano-fibrous materials not only can enhance protein adsorption, but also can promote cells attachment, migration, proliferation and differentiation (Hu, Feng, Liu, & Ma, 2009; Smith, Liu, Hu, & Ma, 2009; Woo, Chen, & Ma, 2003). As a main natural extracellular matrix (ECM) component, collagen does possess a nano-fibrous structure with fiber bundle diameter of from 50 to 500 nm, which plays a pivotal role in the maintenance of cells function in human body (Elsdale & Bard, 1972; Hay, 1991, chap. 7). Hence, engineering materials mimicking the nano-fibrous structure of collagen in the natural ECM is one challenging work in tissue engineering.

To engineer nano-fibrous materials, several technologies such as self-assembly, electrospinning and thermal induced phase separation (TIPS) have been developed (Ma & Zhang, 1999; Matthews, Wnek, Simpson, & Bowlin, 2002; Yu et al., 1999). Self-assembly is currently limited to biological molecules such as peptides with a small fiber diameter of less than 20 nm, and the engineered peptide nano-fibers can be fragmented and may be susceptible to endocytosis (Beniash, Hartgerink, Storrie, & Stupp, 2005). The electrospun fibers often have diameters in the micrometer range, and this technique is also hard to generate designed internal macro pore structure (Ma, 2008). However, phase separation, primarily TIPS, can simultaneously realize both nano-fibrous structure with a fiber diameter of 50–500 nm and designed macro porous architecture (Chen & Ma, 2004). In addition, TIPS technique has good potential in preparing composite nano-fibrous matrices via dual or multiple phase separation processes as well. These exciting advantages make TIPS a very promising way to fabricate biomimetic nano-fibers or 3D nano-fibrous matrices in tissue engineering.

TIPS process takes place from a thermodynamically unstable homogeneous polymer solution tending to separate into a polymer-rich phase and a polymer-lean phase under certain temperature conditions (Ma & Zhang, 1999). After removal of the solvent, the polymer-rich phase solidifies to form the matrix while polymer-lean phase becomes pores. Based on the different phase separation conditions, TIPS may be divided into liquid–liquid phase separation

* Corresponding author at: Department of Materials Science and Engineering, College of Science and Engineering, Jinan University, Guangzhou 510632, China. Tel.: +86 20 85223271; fax: +86 20 85223271.
E-mail address: tumei@jnu.edu.cn (M. Tu).

0144-8617/$ – see front matter © 2010 Elsevier Ltd. All rights reserved.
doi:10.1016/j.carbpol.2010.10.009

Table 1
Preparation conditions and structure of CS matrices by solid–liquid phase separation method.

CS concentration	HAc concentration	[COOH]/[NH_2][a]	Temperature (°C)	Structure[b]
0.05% (w/v)	0.025% (v/v)	1.5	−18	FS
0.05% (w/v)	0.025% (v/v)	1.5	−80	MF
0.05% (w/v)	0.025% (v/v)	1.5	Liquid nitrogen	NF
0.025% (w/v)	0.025% (v/v)	3.0	Liquid nitrogen	NF/FL
0.01% (w/v)	0.025% (v/v)	7.5	Liquid nitrogen	NF/FL
0.05% (w/v)	0.05% (v/v)	3.0	Liquid nitrogen	NF/MF
0.05% (w/v)	0.1% (v/v)	6.0	Liquid nitrogen	NF/MF

[a] Molar ratio of carboxyl groups in acetic acid to amino groups in chitosan.
[b] Four kinds of chitosan acetate structure were included as follows: FS, film-shape; MF, micro-fibers; NF, nano-fibers; FL, floccules-like.

and solid–liquid phase separation. Liquid–liquid phase separation is typical of a polymer solution with an upper critical temperature accompanying the formation of bicontinuous phase structure (polymer-rich and polymer-lean phases), while solid–liquid phase separation displays solvent crystallization from a polymer solution instead (Ma, 2004). In recent years, a number of polymeric nano-fibrous matrices, such as poly(L-lactide), poly(hydroxyalkyl methacrylate)-graft-poly(L-lactide), polyhydroxyalkanoates and gelatin, have been investigated using a liquid–liquid phase separation technique (Li, Zhang, & Chen, 2008; Liu & Ma, 2009, 2010; Ma & Zhang, 1999). The formation and structure of nano-fibrous matrices depend on the gelation of polymer-solvent system which is driven by thermal energy and greatly influenced by temperature, polymer concentration and solvent properties (single or multiple solvent systems). He et al also found that gelation temperature had an influence on the crystallization of poly(L-lactide), and the poly(L-lactide) microcrystalline domains from the gelation could stabilize the polymer-solvent system and prevent further phase separation (He et al., 2009). However, very few researches have been focused on the polymeric nano-fibers preparation by using solid–liquid phase separation approach. The effects of temperature, polymer concentration and solvent properties on the nano-fibrous structure and crystallinity of polymer in the solid–liquid phase separation process have not been known yet.

A variety of synthetic polymeric nano-fibers have been previously engineered by TIPS technique, but few natural macromolecules have been concerned. Chitosan, a copolymer of glucosamine and N-acetylglucosamine derived from the natural polymer chitin, has been attracted much interest in tissue engineering and drug delivery due to its biocompatible, biodegradable, antimicrobial and nontoxic properties (Bhattarai, Edmondson, Veiseh, Matsen, & Zhang, 2005; Lim & Hudson, 2003). In this work, the preparation of chitosan acetate nano-fibers by a solid–liquid phase separation technique has been illustrated. The effects of phase separation temperature, chitosan concentration and acetic concentration on the structure and crystallinity of chitosan acetate matrices have also been investigated.

2. Materials and methods

2.1. Materials

Chitosan (85% deacetylated, viscosity of 1% (w/v) solution in 1% (v/v) acetic acid = 200 cps) was purchased from Shandong Institute of Medical Instruments. All other reagents and solvents used were analytical grade.

2.2. Preparation of chitosan acetate nano-fibers

The preparation of chitosan acetate nano-fibers by solid–liquid phase separation under different phase separation temperature, chitosan concentration, and acetic acid concentration were briefly described as follows:

For the phase separation temperature effect studies, 0.05% (w/v) chitosan solution was prepared by dissolving 5.0 mg chitosan in 10 mL 0.025% (v/v) acetic acid aqueous solution at room temperature. Then, the mixtures were cooled at −18 °C, −80 °C and by soaking in liquid nitrogen respectively for 2 h. The chitosan acetate matrices were obtained by lyophilization at 0.5 mm Hg for 48 h at −80 °C.

For the chitosan concentration effect studies, 0.01%, 0.025% and 0.05% (w/v) chitosan solutions were obtained by dissolving different weight chitosan in a certain volume 0.025% (v/v) acetic acid aqueous solution at room temperature. Subsequently, the mixtures were soaked in liquid nitrogen for 2 h. The chitosan acetate matrices were lyophilized at 0.6 mbar for 48 h at −80 °C.

For the acetic acid concentration effect studies, a series of 0.05% (w/v) chitosan solutions were prepared by dissolving 5.0 mg chitosan in 10 mL acetic acid aqueous solutions of 0.025%, 0.05% and 0.1% (v/v) respectively at room temperature, following by soaking in liquid nitrogen for 2 h. The chitosan acetate matrices were produced after lyophilization at 0.6 mbar for 48 h at −80 °C.

2.3. Characterization

The morphology of chitosan acetate matrices prepared under different preparation conditions was studied by scanning electron microscopy (SEM) (PHILIPSXL-30ESEM). Before SEM analysis, a gold layer was coated on the specimen surface in a sputter coater (BALTEC, SCD005).

The thermal properties of chitosan acetate matrices were analyzed by differential scanning calorimeter (DSC) (NETZSCH DSC 204F1 Phoenix, Germany) in a temperature range from 0 °C to 300 °C with a heating rate of 10 °C/min. The first heating was used for the analysis.

The crystal structure of chitosan acetate matrices was determined by X-ray diffraction (XRD) analysis, which was performed using a X-ray diffractometer (Bruker D8 Focus, Germany) with Cu Kα radiation at a generator voltage of 40 kV and a generator current of 40 mA. Samples were scanned from 2θ = 10–80° at a scanning rate of 8°/min.

3. 3 Results and discussion

3.1. SEM observations

In order to ensure chitosan complete dissolution in acetic acid aqueous solution, excess acetic acid was used based on the stoichiometric calculation of carboxyl groups in acetic acid and amino groups in chitosan, as shown in Table 1. The data summarized in Table 1 showed that temperature, polymer concentration and solvent properties had significant effects on the morphologies of chitosan acetate matrices in the solid–liquid phase separation process. Nano-fibrous, micro-fibrous film-shape and floccules-like structure were formed under different conditions. Uniform nano-fibrous structure could be achieved at an optimal solid–liquid phase

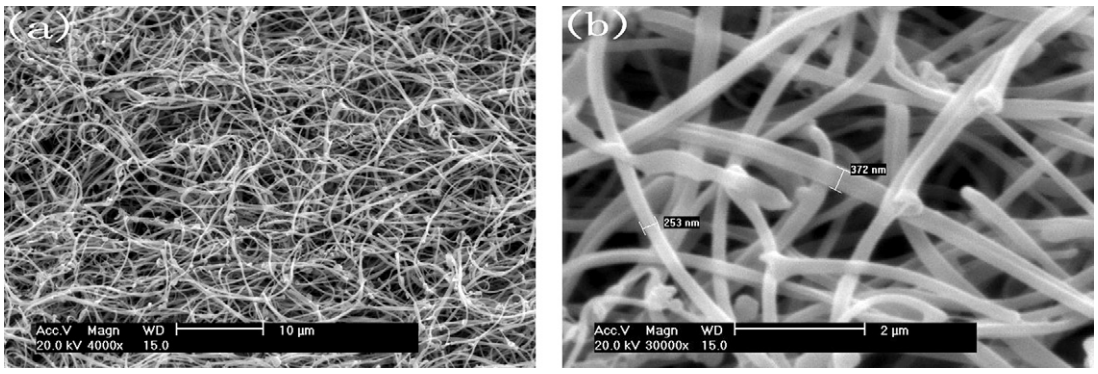

Fig. 1. SEM micrographs of chitosan acetate nano-fibers prepared at 0.05% (w/v) chitosan, 0.025% (v/v) acetic acid and liquid nitrogen: (a) ×4000; (b) ×30,000.

separation condition: 0.05% (m/v) chitosan, 0.025% (v/v) acetic acid and liquid nitrogen environment (Fig. 1). The diameter of nano-fibers ranged from 50 to 500 nm, which is similar to the fibrillar structure of collagen in the natural ECM (Hay, 1991).

A solid–liquid phase separation will take place when a polymer solution is cooled quickly to freeze the solvent and there is not enough time for liquid–liquid phase separation to occur. In this process, the quenching temperature is a key factor in controlling the morphology of resultant polymer matrix because the crystalline morphologies of the polymer and solvent are dependent on the crystallization temperature (Zhang & Ma, 1999). Here, the effects of cooling temperature on the architecture of chitosan acetate matrices were investigated. The freezing point of acetic acid aqueous solution with a concentration range of 0.025% (v/v)–0.1% (v/v) was about −5 °C, which was tested in our lab. When the solutions were cooled down to lower than this temperature, the solubility of chitosan acetate would decrease so that the solid–liquid phase separation process would take place at a certain temperature. The crystallization process includes two stages: nucleation and crystal growth. Generally, a lower temperature induces a higher nucleation rate and a lower crystal growth rate, vice versa (Boyer & Haudin, 2010). The SEM images of chitosan acetate matrices prepared at different quenching temperatures are shown in Fig. 2. Film-shape structure was obtained at −18 °C, which is slightly lower than the freezing point of acetic acid aqueous solution (Fig. 2a); meanwhile, a slow cooling rate leaded to a fast crystal growth and the formation of large chitosan acetate crystals. When a quenching temperature of −80 °C was used, the chitosan solution showed a higher nucleation rate and a slower crystal growth rate than that at −18 °C, and micro-fibrous structure accompanying some small film-shape chitosan acetate matrices was produced (Fig. 2b). Once the chitosan solution was dipped into liquid nitrogen, it would be frozen in a second. The instant nucleation and very slow crystal growth resulted in the formation of nano-fibers with a bundle diameter varying from 50 to 500 nm (Fig. 2 c and d). These results indicated that the supercooling environment in liquid nitrogen was in favor of the formation of uniform nano-scale chitosan acetate fibers. We hypothesized that the formation of nano-fibrous struc-

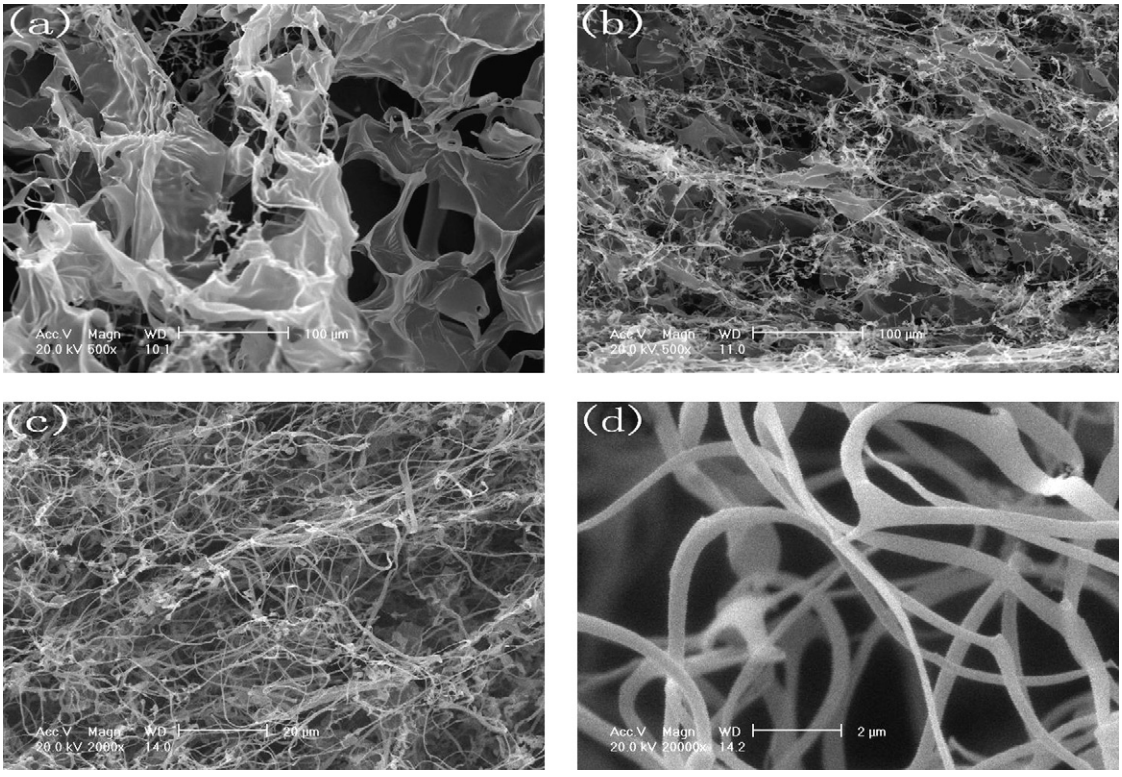

Fig. 2. SEM micrographs of chitosan acetate matrices prepared at 0.05% (w/v) chitosan and 0.025% (v/v) acetic acid using different phase separation temperatures: (a) −18 °C, (b) −80 °C, (c) liquid nitrogen, and (d) enlargement of (c).

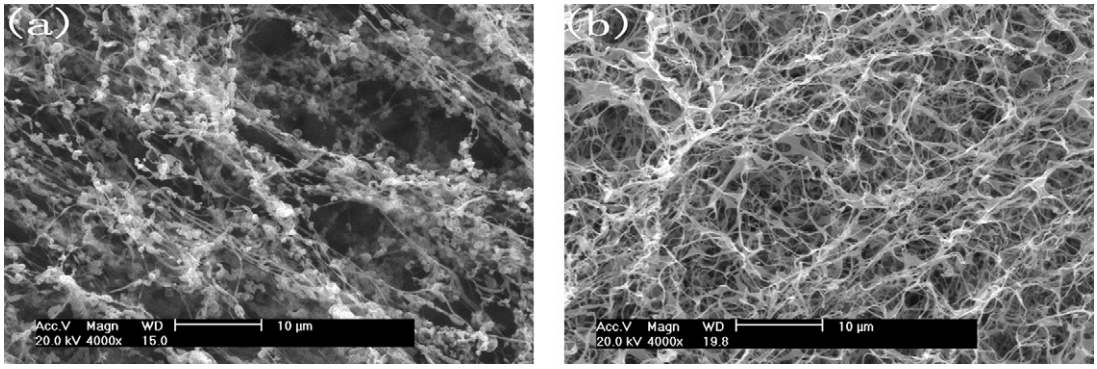

Fig. 3. SEM micrographs of chitosan acetate matrices prepared at different chitosan and acetic acid concentrations under liquid nitrogen: (a) 0.025% (m/v) chitosan and 0.025% (v/v) acetic acid; (b) 0.05% (m/v) chitosan and 0.05% (v/v) acetic acid.

ture was attributed to the sudden freezing of the stretched chitosan acetate molecular chains in a low chitosan concentration solution and the following hyperslow crystal growth rate under liquid nitrogen conditions. In contrast, when the solution was cooled down at a higher temperature of −80 °C or −18 °C, a faster growth of chitosan acetate molecules along the crystal nucleus led to the generation of micro-fibrous or film-shape structure. The phenomenon of chitosan acetate structure significantly changing with quenching temperature is very different from that in liquid–liquid phase separation, where it was considered that the fiber diameter of the matrix did not change with the gelling temperature as long as it was in the fiber-forming temperature range (Ma & Zhang, 1999).

Beside the quenching temperature, the polymer concentration and solvent properties also play a vital role in the polymer crystal morphology (Rogers & Marangoni, 2009; Zhang, Li, Nies, Berghmans, & Ge, 2009). In this work, we studied the effects of chitosan concentration and acetic acid concentration on the structure of chitosan acetate matrices in liquid nitrogen. As mentioned in Fig. 1, uniform nano-fibrous structure could be obtained at a condition of 0.05% (w/v) chitosan and 0.025% (v/v) acetic acid in liquid nitrogen. However, when the chitosan concentration decreased to 0.025% (m/v) or lower, some small floccules occurred on the chitosan acetate nano-fibers surface (Fig. 3a). It might be the reason that in a diluted solution system with an enough low chitosan concentration and excess stoichiometric quantity of acetic acid, the obtained chitosan acetate molecules tended to form random coil, which was responsible for the floccules-like structure during the solid–liquid phase separation process. In contrast, when the chitosan concentration was maintained at 0.05% (m/v) and the concentration of acetic acid aqueous solution was raised to 0.05% (v/v), a very different chitosan acetate morphology of nano-/micro-fibrous structure was engineered comparing with the nano-fibrous/floccules-like structure at 0.025% (m/v) chitosan and 0.025% (v/v) acetic acid even though the molar ratio of [COOH]/[NH_2] was same for both systems (Fig. 3b), but more similar to the nano-fibrous structure obtained at 0.05% (w/v) chitosan and 0.025% (v/v) acetic acid. These results showed that in a certain concentration range of chitosan diluted solution, too low chitosan concentration led to the formation of floccules-like structure while an adequate chitosan concentration was in favor of the generation of nano-fibrous structure instead, which might be relevant to the conformation and distribution of chitosan acetate molecules in the solution. It suggested that the structure of chitosan acetate was more relied on the chitosan concentration than on acetic acid concentration.

3.2. DSC analysis

The glass transition temperature (T_g) and heat capacity (C_p) of chitosan acetate matrices prepared under different conditions were measured by DSC. Fig. 4 showed the first-heating DSC curves of chitosan acetate matrices prepared at optimal chitosan and acetic acid concentration under different quenching temperatures. The DSC thermogram of chitosan acetate control sample showed a broad endothermic peak around 75 °C (Fig. 4a), which might be due to the vaporization of water contaminant in the polysaccharide backbone (Zong, Kimura, Takahashi, & Yamane, 2000). Although chitosan acetate had crystalline regions, the T_g was not found except a decomposition peak around 300 °C because the chitosan acetate backbone had strong inter- and intra-molecular hydrogen bonding (Dong, Ruan, Wang, Zhao, & Bi, 2004). However, by quenching the chitosan solution at different temperatures, the chitosan acetate matrices showed obvious glass transition regions at 150–200 °C. Furthermore, with decreasing the cooling temperature from −18 °C to liquid nitrogen, the T_g reduced from 185.4 °C to 155.1 °C and the corresponding C_p increased from 14.5 J/g to 29.1 J/g instead, as shown in Fig. 4b–d. It could be explained that at a lower quenching temperature, chitosan acetate showed a faster nucleation rate and a slower crystal growth rate, so that more crystallographic defects were generated and there existed more space for chitosan acetate molecule chains to change their conformation. Hence, the chitosan acetate molecules were easier to change the conformation and exhibited a lower T_g when heating; meanwhile more chain segment motion took place and resulted in a higher C_p as well. As mentioned in Section 3.1, nano-fibrous chitosan acetate could be formed in liquid nitrogen instead of film-shape structure at −18 °C. It suggested

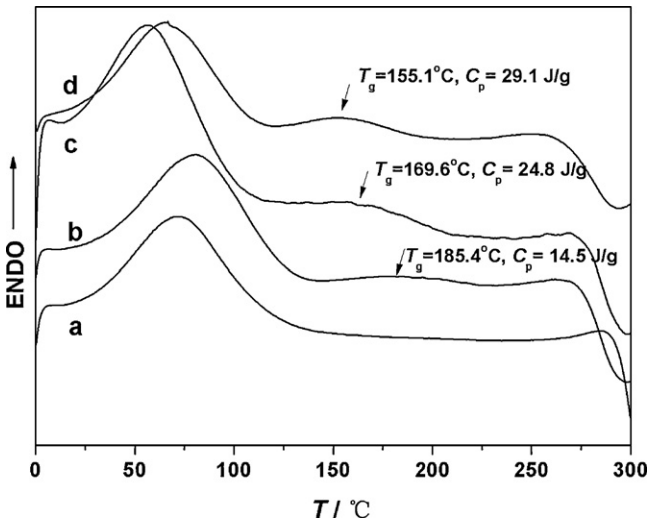

Fig. 4. First-heating DSC curves of chitosan acetate matrices prepared at 0.05% (w/v) chitosan and 0.025% (v/v) acetic acid using different phase separation temperatures: (a) chitosan acetate control; (b) −18 °C; (c) −80 °C; (d) liquid nitrogen.

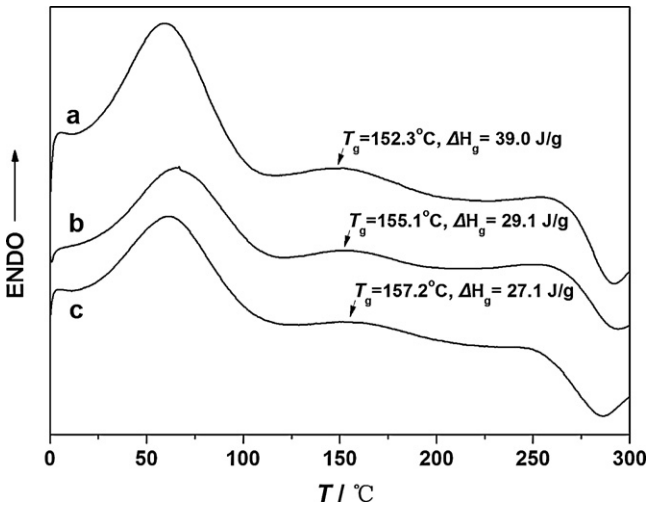

Fig. 5. First-run DSC curves of chitosan acetate matrices prepared at different chitosan and acetic acid concentrations under liquid nitrogen: (a) 0.025% (m/v) chitosan and 0.025% (v/v) acetic acid; (b) 0.05% (m/v) chitosan and 0.025% (v/v) acetic acid; (c) 0.05% (m/v) chitosan and 0.05% (v/v) acetic acid.

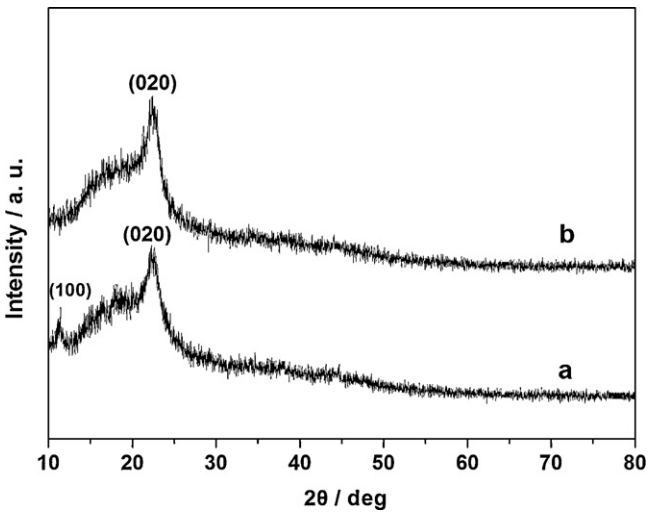

Fig. 6. XRD patterns of chitosan acetate matrices: (a) chitosan acetate control; (b) prepared at 0.05% (w/v) chitosan, 0.025% (v/v) acetic acid and liquid nitrogen.

that the crystallinity of chitosan acetate significantly affected by the cooling temperature was responsible for the product structure fabricated at different temperatures. The formation of nano-fibrous chitosan acetate should be owed to its lower crystallinity prepared in liquid nitrogen.

As described in Section 3.1, the concentration of chitosan and acetic acid had an effect on the structure of chitosan acetate during the solid–liquid phase separation. The influence of chitosan concentration and acetic acid concentration on the thermal properties of chitosan acetate matrices was also studied, as shown in Fig. 5. All the first-heating DSC curves exhibited a visible glass transition region around 150 °C. For the sample with uniform nano-fibrous structure prepared at the optimal conditions of 0.05% (w/v) chitosan and 0.025% (v/v) acetic acid in liquid nitrogen, chitosan acetate showed a T_g of 155.1 °C and a C_p of 29.1 J/g, whereas at a lower chitosan concentration of 0.025% (w/v), a lower T_g of 152.3 °C and a higher C_p of 39.0 J/g were obtained. It was possible that the relatively imperfect chitosan acetate crystals formed at a lower chitosan concentration leaded to a lower T_g and a higher C_p since a sample with a lower crystallinity usually possesses a lower T_g and a higher C_p (Schick, 2009). In contrast, when keeping the chitosan concentration at 0.05% (w/v) and increasing the acetic acid concentration to 0.05% (v/v), the chitosan acetate presented a higher T_g of 157.2 °C and a lower C_p of 27.1 J/g instead, which were closer to the T_g and C_p values at 0.05% (w/v) chitosan and 0.025% (v/v) acetic acid than those obtained at 0.025% (w/v) chitosan and 0.025% (v/v) acetic acid. These results indicated the crystallinity of chitosan acetate was more dependent on the chitosan concentration than on the acetic acid concentration. Furthermore, a higher chitosan concentration was beneficial to produce higher T_g and lower C_p maybe attributing to the formation of relatively perfect chitosan acetate crystals. The effect of chitosan concentration and acetic acid concentration on the crystallinity of chitosan acetate was in accordance with that on the structure of chitosan acetate. Hence, it can be deduced that the structure of chitosan acetate formed in the solid–liquid phase separation was correlative to the crystallinity of chitosan acetate.

3.3. XRD analysis

The XRD patterns of chitosan acetate matrices before and after solid–liquid phase separation were shown in Fig. 6. Before solid–liquid phase separation, the peaks of chitosan acetate at around $2\theta = 11.4^\circ$ and 22.0° were attributed to the diffraction from the chitosan acetate crystal planes of (1 0 0) and (0 2 0) respectively (Fig. 6a) (Zeng et al., 2009). According to the previous report, the reflection at $2\theta = 11.4^\circ$ assigned to crystal form I and the stronger reflection appeared at $2\theta = 22.0^\circ$ corresponded to crystal form II (Ma, Qian, Yang, Hu, & Nie, 2010). However, in the patterns of chitosan acetate matrices after solid–liquid phase separation in liquid nitrogen, the (1 0 0) reflection peak disappeared and the (0 2 0) reflection peak was slightly strengthen (Fig. 6b). It seemed that the crystal form I of chitosan acetate was changed to crystal form II after solid–liquid phase separation. It might be ascribed to the chitosan acetate chain structure changes between chitosan acetate flake state and quenching state from chitosan solution (Zong, Kimura, Takahashi, & Yamane, 2000).

4. Conclusions

Various chitosan acetate structure, i.e. nano-fibrous, micro-fibrous, film-shape and floccules-like, were generated by solid–liquid phase separation, which was dramatically influenced by the phase separation temperature, chitosan concentration as well as acetic acid concentration. Phase separation temperature was the predominant factor of chitosan acetate structure. A lower quenching temperature facilitated the formation of nano-fibrous structure; meanwhile the structure of chitosan acetate was more affected by the chitosan concentration than by the acetic acid concentration. Uniform chitosan acetate nano-fibers with a bundle diameter range of 50–500 nm could be engineered under optimal conditions of 0.05% (w/v) chitosan, 0.025% (v/v) acetic acid and liquid nitrogen. The phase separation conditions had a significant effect on the crystallinity of chitosan acetate matrices, which was responsible for product structure obtained by solid–liquid phase separation, and a lower crystallinity was in favor of the formation of nano-fibrous structure. Furthermore, chitosan acetate crystal form was also changed from I to II after solid–liquid phase separation in liquid nitrogen. Hence, the structure and crystallinity of polymer can be regulated by solid–liquid phase separation technique, which will be a potential tool to fabricate nano-fibrous structure for tissue engineering materials.

Acknowledgements

The authors are thankful to financial support from the National High Technology Research and Development Program of China (863 Program) (No. 2007AA09Z440) and the National Natural Science Foundation of China (No. 30900296).

References

Beniash, E., Hartgerink, J. D., Storrie, H., & Stupp, S. I. (2005). Self-assembling peptide amphiphile nanofiber matrices for cell entrapment. *Acta Biomaterialia*, *1*, 387–397.

Bhattarai, N., Edmondson, D., Veiseh, O., Matsen, F. A., & Zhang, M. (2005). Electrospun chitosan-based nanofibers and their cellular compatibility. *Biomaterials*, *26*, 6176–6184.

Boyer, S. A. E., & Haudin, J. M. (2010). Crystallization of polymers at constant and high cooling rates: A new hot-stage microscopy set-up. *Polymer Testing*, *29*, 445–452.

Chen, V. J., & Ma, P. X. (2004). Nano-fibrous poly(L-lactic acid) scaffolds with interconnected spherical macropores. *Biomaterials*, *25*, 2065–2073.

Dong, Y. M., Ruan, Y. H., Wang, H. W., Zhao, Y. G., & Bi, D. X. (2004). Studies on glass transition temperature of chitosan with four techniques. *Journal of Applied Polymer Science*, *93*, 1553–1558.

Elsdale, T., & Bard, J. (1972). Collagen substrata for studies on cell behavior. *Journal of Cell Biology*, *54*, 626–637.

Hay, E. D. (1991). *Cell biology of extracellular matrix* (2nd ed.). New York: Plenum Press.

He, L. M., Zhang, Y. Q., Zeng, X., Quan, D. P., Liao, S. S., Zeng, Y. S., et al. (2009). Fabrication and characterization of poly(L-lactic acid) 3D nanofibrous scaffolds with controlled architecture by liquid–liquid phase separation from a ternary polymer-solvent system. *Polymer*, *50*, 4128–4138.

Hu, J., Feng, K., Liu, X. H., & Ma, P. X. (2009). Chondrogenic and osteogenic differentiations of human bone marrow-derived mesenchymal stem cells on a nanofibrous scaffold with designed pore network. *Biomaterials*, *30*, 5061–5067.

Li, X. T., Zhang, Y., & Chen, G. Q. (2008). Nanofibrous polyhydroxyalkanoate matrices as cell growth supporting materials. *Biomaterials*, *29*, 3720–3728.

Lim, S. H., & Hudson, S. M. (2003). Review of chitosan and its derivatives as antimicrobial agents and their uses as textile chemicals. *Journal of Macromolecular Science Polymer Reviews*, *C43*, 223–269.

Liu, X. H., & Ma, P. X. (2009). Phase separation, pore structure, and properties of nanofibrous gelatin scaffolds. *Biomaterials*, *30*, 4094–4103.

Liu, X. H., & Ma, P. X. (2010). The nanofibrous architecture of poly(L-lactic acid)-based functional copolymers. *Biomaterials*, *31*, 259–269.

Ma, P. X. (2004). Scaffolds for tissue fabrication. *Materials Today*, *7*, 30–40.

Ma, P. X. (2008). Biomimetic materials for tissue engineering. *Advanced Drug Delivery Reviews*, *60*, 184–198.

Ma, P. X., & Zhang, R. Y. (1999). Synthetic nano-scale fibrous extracellular matrix. *Journal of Biomedical Materials Research*, *46*, 60–72.

Ma, G. P., Qian, B., Yang, J. X., Hu, C. Q., & Nie, J. (2010). Synthesis and properties of photosensitive chitosan derivatives(1). *International Journal of Biological Macromolecules*, *46*, 558–561.

Matthews, J. A., Wnek, G. E., Simpson, D. G., & Bowlin, G. L. (2002). Electrospinning of collagen nanofibers. *Biomacromolecules*, *3*, 232–238.

Rogers, M. A., & Marangoni, A. G. (2009). Solvent-modulated nucleation and crystallization kinetics of 12-hydroxystearic acid: A nonisothermal approach. *Langmuir*, *25*, 8556–8566.

Sahoo, S., Ang, L. T., Goh, J. C. H., & Toh, S. L. (2010). Growth factor delivery through electrospun nanofibers in scaffolds for tissue engineering applications. *Journal of Biomedical Materials Research*, *93A*, 1539–1550.

Schick, C. (2009). Differential scanning calorimetry (DSC) of semicrystalline polymers. *Analytical and Bioanalytical Chemistry*, *395*, 1589–1611.

Smith, L. A., Liu, X. H., Hu, J., & Ma, P. X. (2009). The influence of three-dimensional nanofibrous scaffolds on the osteogenic differentiation of embryonic stem cells. *Biomaterials*, *30*, 2516–2522.

Wei, G. B., & Ma, P. X. (2008). Nanostructured biomaterials for regeneration. *Advanced Functional Materials*, *18*, 3568–3582.

Woo, K. M., Chen, V. J., & Ma, P. X. (2003). Nano-fibrous scaffolding architecture selectively enhances protein adsorption contributing to cell attachment. *Journal of Biomedical Materials Research*, *67A*, 531–537.

Yu, Y. C., Roontga, V., Daragan, V. A., Mayo, K. H., Tirrell, M., & Fields, G. B. (1999). Structure and dynamics of peptide-amphiphiles incorporating triple helical protein like molecular architecture. *Biochemistry*, *38*, 1659–1668.

Zeng, R., Tu, M., Liu, H. W., Zhao, J. H., Zha, Z. G., & Zhou, C. R. (2009). Preparation, structure, drug release and bioinspired mineralization of chitosan-based nanocomplexes for bone tissue engineering. *Carbohydrate Polymers*, *78*, 107–111.

Zhang, R. Y., & Ma, P. X. (1999). Poly(α-hydroxyl acids)/hydroxyapatite porous composites for bone-tissue engineering. I. Preparation and morphology. *Journal of Biomedical Materials Research*, *44*, 446–455.

Zhang, T. Z., Li, T., Nies, E., Berghmans, H., & Ge, L. Q. (2009). Isothermal crystallization study on aqueous solution of poly(vinyl methylether) by DSC method. *Polymer*, *50*, 1206–1213.

Zhao, Y., Tanaka, M., Kinoshita, T., Higuchi, M., & Tan, T. W. (2010). Nanofibrous scaffold from self-assembly of beta-sheet peptides containing phenylalanine for controlled release. *Journal of Controlled Release*, *142*, 354–360.

Zong, Z., Kimura, Y., Takahashi, M., & Yamane, H. (2000). Characterization of chemical and solid state structures of acylated chitosans. *Polymer*, *41*, 899–906.